Forecasting the Temperature of BEV Battery Pack Based on Field Testing Data

Ka Seng Chou[1,2(✉)], Kei Long Wong[1], Davide Aguiari[2,3], Rita Tse[1], Su-Kit Tang[1], and Giovanni Pau[2,3,4]

[1] Faculty of Applied Sciences, Macao Polytechnic University, Macao SAR, China
{kaseng.chou,keilong.wong,ritatse,sktang}@mpu.edu.mo
[2] Department of Computer Science and Engineering, Alma Mater Studiorum, University of Bologna, Bologna, Italy
{davide.aguiari2,giovanni.pau}@unibo.it
[3] Autonomous Robotics Research Center, Technology Innovation Institute, Abu Dhabi, UAE
[4] UCLA Samueli Computer Science, University of California, Los Angeles, Los Angeles, USA

Abstract. Monitoring electric vehicles' battery situation and indicating the state of health is still challenging. Temperature is one of the critical factors determining battery degradation over time. We have collected more than 2.3 million discharging samples via a custom Internet of Thing device for more than one year to build a machine-learning model that can forecast the battery pack's average temperature in real-world driving. Our best Bi-LSTM model achieved the mean absolute error of 2.92 °C on test data and 1.7 °C on cross-validation for prediction of 10 min on the battery pack's temperature.

Keywords: Electric Vehicle · Battery Temperature Forecasts · Electric Vehicle Data · Lithium-ion Battery · Driving Behaviour · Machine Learning

1 Introduction

Battery electric vehicles (BEVs) battery pack temperature monitoring and control is vital for the longevity of the Li-ion batteries (LiBs) life. The essential measurement of the battery pack's internal temperature (IT) is to prevent thermal runaway and the batteries burst into flames for the BEV [12] in autonomous driving area [4]. To increase safety and prolong the LiBs' life, the Battery Management System (BMS) keeps measuring the pack temperature constantly [11]. Based on the geometrical layout of the LiBs' pack, multiple thermistors are deployed at different spots inside the LiBs' container to acquire the precise temperature. However, the performance of this temperature sensing method inevitably depends on the thermal conduction of the individual LiB cell and the pack-based cooling medium (i.e., air, liquid, and phase change materials) [19,24,26].

Z. Xiao et al. (Eds.): ICECI 2022, LNICST 478, pp. 3–17, 2023.
https://doi.org/10.1007/978-3-031-28990-3_1

Meanwhile, the LiB's cells wiring structure (i.e., cells parallel and series connection) also affects the temperature of the modules, which causes some cells to have a higher temperature than the others [5,28]. Likewise, measuring the current temperature of the battery pack is not enough because the thermal delay effect exists from LiB's core to the surface, cell to cell, and finally to the temperature sensors [27]. Therefore, forecasting the temperature during the battery becomes the problem solver for the major degradation of LiBs.

For temperature predictions, existing statistical models are already capable of making a single prediction. For example, the statistical Hidden Markov Model (HMM), the Support Vector Regression (SVR) model, the linear model, and the decision tree for temperature prediction [18,25]. However, these models are not able to predict or represent temperature over time when human factors are involved.

In recent years, machine learning has been used to predict the batteries-related temperature for the BEVs at different portions inside the battery pack. In research from Jaliliantabar et al. [15], an artificial neural network (ANN) is equipped with the phase change materials (PCM) based battery thermal management system (BTMS) to predict the LiBs temperature in different operating conditions by the input of charging rate, PCM type, PCM thickness, and time. Fang et al. [10] used the ANN model to predict the nickel-metal hydride battery surface temperature with the input of ambient temperature, charging rate, and charging time. To predict the discharging temperature, Jiang et al. [16] used the long short-term memory-recurrent neural network (LSTM-RNN) and gated recurrent unit-recurrent neural network (GRU-RNN) to effectively estimate the surface temperature within a maximum absolute error of 0.75 °C.

There are many other studies to forecast the battery system's temperate in different ways for the BMS, including physical, electrochemical, or thermodynamics model [3,9,22]. However, the real-world daily use of the BEV is nonlinear and dynamic. This involves much more complicated factors such as the differential from manufacturing, drivers driving behavior, and the temperature climate [6,7,14,21]. For this reason, we collected around 168 h of driving data from an EV in Bologna (Italy) via an IoT device attached to its control units.

This study aims to develop an ANN that effectively keeps drivers aware of the battery temperature conditions in the edge. This network best represents the connection between the LiB pack's temperature and all the feasible corrected input from the IoT device. In specific, the contributions of this study are as follows:

1. a systematic analysis and resampling of the updated real-world collected *Nissan Leaf 2018 EV* driving dataset introduced in [1];
2. development of the neural network for evaluating the Nissan Leaf battery discharge heat dissipation against the optimal temperature range for the edge computing;

The paper is organized as follows: Sect. 2 is an overview of the data collection, in which the IoT device and *Nissan Leaf* battery pack's structure are described. Section 3 focuses on the data preprocessing and feature selection of the collected

results from real-world driving. Section 4 describes the method to search for the best neural network and the training environment. The Sect. 5 discusses the results and implications from Optuna tuning and the importance of some weights. Finally, some future improvements are provided in the final section.

2 Approach

2.1 The IoT Device

To gather the ECUs data from the *Nissan Leaf* 2018 model, we used the low-cost IoT device described in [1]. In short, it is an On-Board Diagnostic version II (OBD2) LTE-connected reader that queries the Leaf's Vehicle Control Module at 250 ms intervals continuously. Several parameters are collected and clustered according to their category (i.e. HV battery data, such as its current and voltage at pack level up to its 96 cells voltage; HVAC data, such as cabin and ambient temperature, A/C and its energy consumption; driver's behavior, such as pressure on both acceleration pedal and brake pedal, the car's speed, etc.). The optimal temperature window for a single LiB cell is from 15 °C to 35 °C [14]. According to the SOC, this window has a slight variety corresponding to the cell voltage from 2.5 V (empty) to 4.2 V (fully charged) [13,20]. Figure 1 shows the *Nissan Leaf*'s battery pack which is analyzed to obtain the temperature voltage window. There are twenty-four sub-modules in Leaf's battery pack. Each sub-module consists of eight cells arranged in two units with two sets of two parallel cells. The total voltage is 350 V when all the sub-modules are serialized which is equal to two cells in parallel and 96 sets in series. With this battery pack

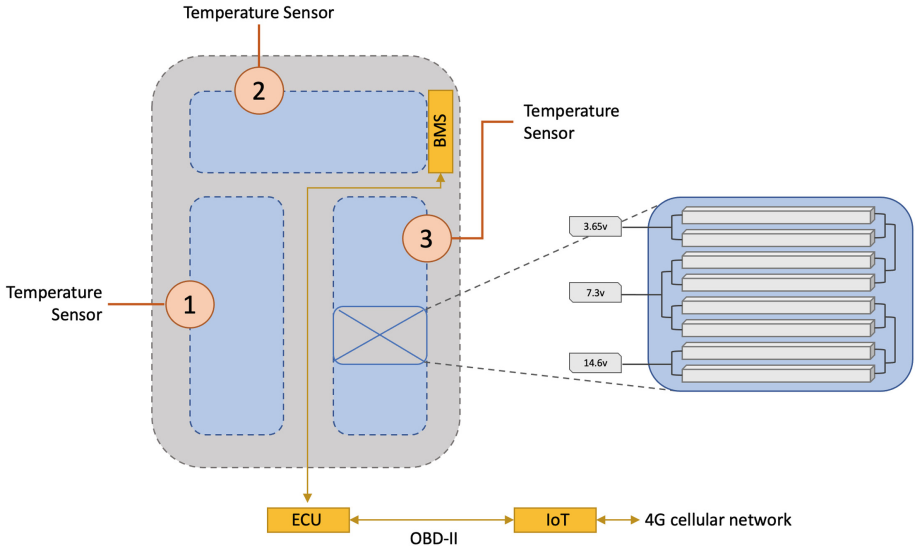

Fig. 1. The structure of the cells in *Nissan Leaf* [17]

structure, the voltage center is shifted to 350 V which is 96 times larger than a single cell. Therefore, the Leaf's temperature voltage window is ranging from 250 V to 450 V.

3 Data Preparation

3.1 Data Cleansing

The full dataset is preprocessed with the following steps for the dataset:

1. selected the test vehicle raw discharge data from 2020-01-09 to 2022-08-03. The total number of rows was 2.4 million (i.e., 168 h);
2. calculation with indirect variables (i.e. instant power, charging power, remaining power, acceleration, and horsepower) for all records;
3. identified and labeled if any, different groups of trips that may exist on a single day with different stopping intervals or different drivers;
4. clustered and labeled different trips: we targeted the power on button, the charging plug state, and the charging mode on the vehicle. We consider a trip which is a set of records that lasts more than 30 min;

All the non-behavior-related features are removed since not all the collected features from the BEV are related to the High-Voltage (HV) battery output. The features (e.g., headlights, fan speed, wipers, etc.) that are powered by the 12 V battery are ignored.

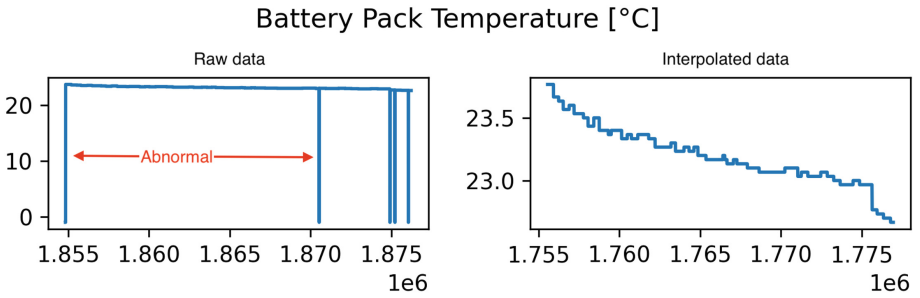

Fig. 2. The bidirectional linear interpolation of null and missing values

Figure 2 shows the interpolation of the battery pack temperature in a trip. The bidirectional linear interpolation is applied to address the missing and null values. Trip-based z-score filtering is adopted to filter out the out-liners. For any values in a feature, the z-score larger than 3 (covered 99% of the data) is set to null and interpolated. Any other abnormal values are interpolated if we identified any. The general summary of the high-quality discharge dataset (∼130 h) for the machine learning task is shown in Table 1.

Table 1. The summary of filtered discharging dataset

	Odometer	SOC	SOH	Voltage	Current*	Ambient °C
count	1918299	1918299	1918299	1918299	1918299	1918299
mean	9217.46	74.72	94.41	373.31	-22.47	18.65
std	3213.64	19.16	1.38	19.68	38.49	8.29
min	255	0.32	92.63	0	-370.67	3.5
25%	6673	61.2	93.06	356.13	-39.22	12
50%	9431	78.99	93.91	374.95	-5.59	17
75%	11890	91.39	95.88	391.41	-0.98	24
max	15537	99.11	96.46	655.35	179.66	44.5
Interpolated [%]	3.52	1.31	0.79	0.05	0.05	0
(continued)	Pack 1 °C	Pack 2 °C	Pack 4 °C	All Packs Avg. °C		
count	1918299	1918299	1918299	1918299		
mean	24.95	24.87	23.34	24.39		
std	9.14	8.82	8.11	8.66		
min	5.8	5.6	5.76	5.83		
25%	17.3	17.45	16.4	17.1		
50%	25.2	25.1	23.3	24.7		
75%	32	31.44	29.44	30.97		
max	55	54	48.4	52.47		
Interpolated [%]	0.02	0.02	0.02	0.02		

*The current load is negative when discharging (driving) and positive when regenerative braking.

3.2 Feature Engineering

Data Resampling certain driving-related factors are accumulated due to the long sampling rate on the battery pack's temperature. The fastest temperature sampling rate is about 60 to 90 s after the test on the *Nissan Leaf*. If the 250 ms data is input directly to the machine learning (ML) algorithms, it will cause a non-effective prediction of the results. This means the loss of the ML models would be low, which is repeating the same output values but not effectively predicting the minor changes in the temperature. Figure 3 shows a one-minute resample of the data. Noticing that the simple resample would lose the fine-time granularity meaning of the dataset, we accumulated the driving relational features to compensate for the loss.

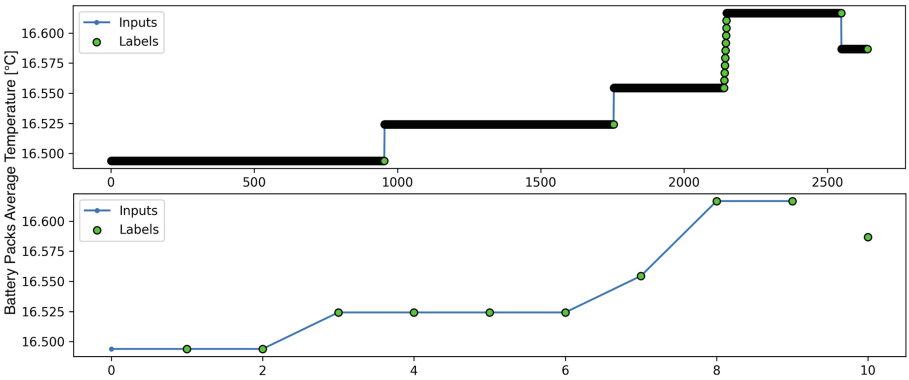

Fig. 3. The temperature sample in 10 min

On every trip, the value of these variables (i.e., accelerator pedal, braking pedal, speed, etc.) grows at the BEV start-up as the extra features. From a training input point of view, a constant accumulation operation is closer to a battery's operating principle, a consequence of a chain reaction from driving manners. Also, Xu et al. [29] revealed that the discrete incremental capacity can improve the estimation accuracy of SOH. Therefore, these features are processed to accumulate at the beginning of every trip.

Cyclical Encoding the timestamp data is encoded into a cyclical representation of a particular day, season, and year with sine (1) and cosine (2) [23]. A total of six new cyclical features (i.e., day sine and cosine, season sine and cosine, year sine and cosine) have been added to emphasize the temperature climate for the ANN.

$$\text{Periodic sine} = \sin\left(timestamp \times \frac{2\pi}{period}\right) \tag{1}$$

$$\text{Periodic cosine} = \cos\left(timestamp \times \frac{2\pi}{period}\right) \tag{2}$$

where:

$$\text{period} = \begin{cases} \text{day} & 24 \times 60 \times 60 \\ \text{season} & 91.31 \times day \\ \text{year} & 365.24 \times day \end{cases}$$

3.3 Data Windowing

The input and output window size is set to 10 (i.e. 10 min). Summarised from the dataset, the average cool-down time for the entire battery pack is approximately 10 to 15 min at 1 °C when driving. The output window size of 10 gives the driver sufficient time to ameliorate the driving behaviors or conditions for the drivers, which is intended to keep the battery pack's temperature in better condition.

To enable the many-to-many predictions of the model, trip data is sliced into the size window for both the input and output for the model training. This consecutive windowing allows the model to predict the next x minutes, based on the current x minutes. The following Fig. 4 demonstrated the construction of ten-time steps of the input and output labels from the dataset. A shuffleable batch of input is generated by sliding the window for the next one-time step. The different NNs (e.g., linear network, LSTM) are processed propinquity to satisfy the network input shape requirements. Finally, the data is split into 70% for training, 20% for validation, and 10% for testing.

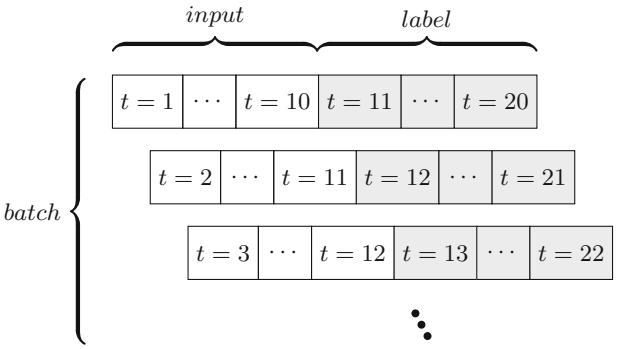

Fig. 4. The consecutive many-to-many window training input for ANN.

4 Models

This section detailed the search method of our best LSTM model for predicting the battery pack's temperature.

4.1 Model Defines

The LSTM model is built in favor of simplicity because of lesser features and reprocessed. Also, the battery temperature prediction tends to perform better in the simple model with less past status by the temperature characteristic [10,15]. In the model evaluation, the Mean Absolute Error (MAE) (4) is adopted. To prevent overfitting of simple machine learning models, L2 regularization (5) is added into the MSE loss function to penalize models.

$$\mathrm{MSE} = \frac{1}{n}\sum_{i=1}^{n}(y_{i,t} - y_{i,p})^2 \tag{3}$$

$$\mathrm{MAE} = \frac{1}{n}\sum_{i=1}^{n}|y_{i,t} - y_{i,p}| \tag{4}$$

$$\mathrm{L2} = \lambda \sum_{i=1}^{n} {w_i}^2 \tag{5}$$

where the $y_{i,t}$, $y_{i,p}$, and n are target value, predicted value, and number of samples in the dataset.

4.2 Hyperparameter Searching

To construct the network and hyperparameter tuning, Optuna is adopted. It is a neural network optimization framework that automates the searching and pruning strategy for different networks [2]. Compared to the grid search and random search, Optuna can reduce the computational resources significantly and better locate the minima. Figure 5 shows the overall structure of the Optuna. Firstly, the three dimension input is reshaped into the batch and the vector of window size times features as the input to the Optuna. The Optuna framework then searches automatically for the best number of layers, neurons, and regularization for the intermediate network. A fully connected (FC) layer is attached after Optuna to convert the different network settings to a constant shape. Finally, the FC layer is reshaped to the output window shape.

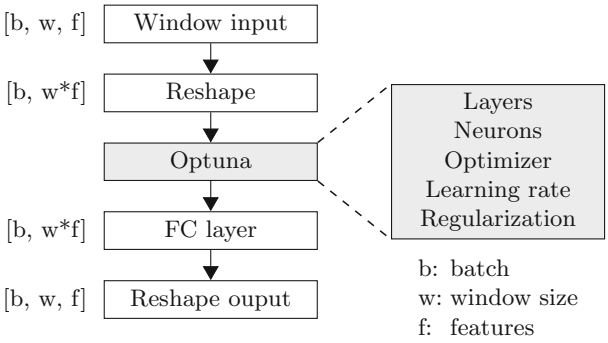

Fig. 5. Optuna framework structure for automatic search and network construction.

Table 2. The Optuna automatic search settings

Optuna	Settings
Max. searches	1,000
Max. layers	10
Neurons	4 to 512
Optimizer	Adam, SGD, RMSProp
Learning rate	1e-5 to 1e-1
Regularization	1e-10 to 1e-3

Table 2 shows the detailed searching parameters setting inside the Optuna layers. The activation and initialization are fixed to Relu and He uniform variance to reduce the searching time. The search of hyperparameter combinations is set to 1,000 for the model. The following Table 3 shows the settings of our best model.

Table 3. The Best Model - Bidirectional LSTM

	Settings
Layers	3
Structure	Bi-LSTM(341) x Bi-LSTM(32) x FC(420)
Optimizer	Adam
Learning rate	6.48E-05
Regularization	1.33E-10
Early stopping	with validation loss
Total parameters	1,257,892

5 Results and Discussion

In this section, the results and implications of our best model are presented. The different datasets and models are compared to identify the most important factors for temperature prediction. The ablation study on the features was also included to verify the importance of feature engineering. The limitations and considerations of our work are also discussed. Finally, the consequences of the capacity loss caused by temperature are explained.

5.1 Justification of the Best Model

The MAE on the prediction of the average temperature of the battery pack is the performance indicator for all models. Table 4 shows the different model comparisons using the test data (10%) and a 10-fold cross-validation. Two output variables are tested that are associated with the constant input of 10 window

Table 4. The MAE benchmarking [°C]

Models	10 Predictions	10-Fold-10	1 Prediction	10-Fold-1
CNN	7.69	7.36	-	-
MLP	7.69	7.35	7.9	7.33
Linear	13.2	12.16	14.74	13.29
LSTM	3.16	2.12	4.14	3.21
Bi-LSTM	2.92	1.7	2.83	2.06

steps: (i) the output of 10 temperature predictions (10 min) which is our main goal; (ii) the output of a single temperature prediction in the last minutes of the 10 min as a reference.

The Bi-LSTM model showed the smallest error of 2.92 °C in the test data and a mean error of 1.7 °C in the cross-validation of the 10 predictions output. When these two errors are averaged, an error of 2.31 °C is the best performance we found for this model. The multi-window linear model showed the worst performance among the models. There is almost no difference in the prediction errors between the CNN and MLP models. For reference, the model with one output shows similar performance. The CNN model is not available for single output due to the restriction to a minimum dimension.

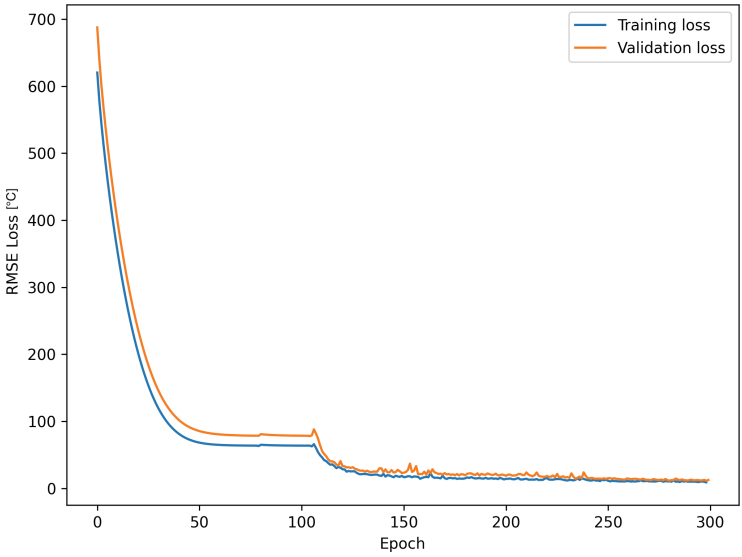

Fig. 6. Training loss on the best model

The training and validation loss is shown in Fig. 6. The training of the model converges smoothly in the first 300 epochs with a time cost of about 2400 s. The validation loss of the model gradually decreases and overlaps with the training loss at epoch 250.

5.2 Ablation Study

The ablation study focuses on the features, as Optuna had sought the optimal structure for the model, which is a standard model without adjustments. Table 5 shows the result of removing accumulated variables, time signals, both accumulated variables and time signals, and trip labels.

Table 5. The MAE on features ablation

Remove	MAE [°C]	10-Fold-10 [°C]
ACC. features	7.69	7.36
Time	3.87	3.87
ACC. and Time	7.69	7.36
Trip label	3.5	3.29

We have found that the accumulated characteristics are of significant importance. When removed, the MAE increases to 7.69 °C. This shows that the Bi-LSTM model is partially based on the linear signal. When the time signal is removed, the MAE of the model increases by about 1 °C. Based on the model results, temporal variations (e.g., seasonal factors or road conditions) also affect the temperature of the battery pack. Finally, the temperature increases by about 0.6 °C when a trip number is removed. In addition, we recorded an MAE increase to 4.41 °C and a 10-fold validation of 2.17 °C when adding the driver ID as a feature.

5.3 Dataset Comparison

To our knowledge, this is the only dataset collected without simulation or modeling on a real *Nissan Leaf's* ECU. Instead of comparing the model to the existing dataset, we compare it to the new dataset assembled from our data. It is because the above feature ablation study shows the importance of features. Also, it may not be comprehensive enough to compare performance with the different battery types, cells, and laboratory-tested datasets [8]. This resampled dataset follows China's mandatory electric vehicle data collection protocol GB/T 32960.3 and our feature engineering steps. The difference between the GB/T 32960 dataset and ours is the sampling rate of 30 s.

Table 6 shows a very small loss of precision in both MAE and 10-fold validation when predicting 10 outputs. Compared to our 250 ms fine-time granularity, the Bi-LSTM model still performs effectively at the 30 s interval for temperature prediction on the battery pack.

Table 6. The MAE difference on the Chinese standard

Dataset	MAE [°C]	10-Fold-10 [°C]
30 s resampled	3.57	1.76
Ours	2.92	1.7
Difference	0.65	0.06

5.4 Statistical Learning Comparison

To understand the performance of our data, statistical learning models are compared. Four one-to-one models, including Support Vector Regression (SVR) with Gaussian kernel, linear, Ada Boost Regressor and Decision Tree Regressor, are implemented to test the prediction errors. The ratio of training and testing is set to 0.67 and 0.33, respectively. Table 7 shows that the linear model achieves the minimum MAE error of 0.41 °C. However, this result cannot be directly compared with our model because it cannot detect the input in the next x minutes.

Table 7. The MAE of the statistical learning approach

Models	MAE [°C]
SVR-Gaussian	6.0258
Linear	0.4058
Ada Boost Regressor	0.612
Decision Tree Regressor	0.8109

5.5 Limitations and Reflection

In this model, we focus on temperature prediction in the edge for the battery packs. Considering the lower computational power in the edge, we did not further address the modeling of driving behavior or user behavior. Infact, other feature extensions can be tried, including higher-order features, factorization machines, or retrieval pools. The performance can potentially be higher than the current model if we apply these behavior modeling techniques instead of simple feature accumulation.

5.6 Capacity Fading

Generally, the optimal temperature range for LiBs is from 15 °C to 35 °C [14]. Jia et al. show the 19.2% capacity fading in Worldwide harmonized Light vehicles Test Cycles at 45 °C after 2,184 cycles [13]. The electrochemistry degradation mechanisms are as followings:

High Temperature when temperature increases at a high voltage and SOC, the electrolyte decomposes and forms gas. Cracks would appear in the cathode, forming an unstable structure that blocks the Li-ion stream and causes capacity fading. Dendrites grow on the anode, which can pierce the separator.

Low Temperature slowing the Li-ion diffusion which causes lithium plating and metalization on the anode and consumes the Li-ion.

By evaluating the performance of these models, it can be concluded that the performance of the EV battery pack's temperature forecasting depends mainly on the model's type. Instead of a complex model and heavy load of training,

a simple Bi-LSTM model is the most appropriate depending on our data and possibly the China's GB/T 32960.3 standard EV data. This simple model may also be applied to the EV's ECUs to assist the LiBs' thermal management and the driver.

6 Concluding Remark

In this work, a EV-LiB temperature prediction model was built in a data-driven way including data acquisition, preprocessing, and modeling. From the OBD2 IoT sensor, we processed more than 2.3 million (i.e., 160 h) update to date discharge samples from the *Nissan Leaf* with a sampling rate of 250 ms. The data is filtered and converted into a time series window, with the time signal catering to the machine learning models for many-to-many prediction. For the data with fine temporal granularity, a simple Bi-LSTM model showed the best performance compared to the previous work on the dense model. The model also exhibited similar performance on our reproduced dataset by following the Chinese protocol GB/T 32960.3. Illustrating from the models, the temperature of LiBs is affected by successive driving behaviors, temporal signals, trips, and drivers. In addition, due to the simplicity of this model, it is also possible to act on the EV's control unit to best control the optimal temperature of the battery to extend the battery life.

Acknowledgements. This work was supported in part by the Macao Polytechnic University - Edge Sensing and Computing: Enabling Human-centric (Sustainable) Smart Cities (RP/ESCA-01/2020) and by the H2020 project titled "European Bus Rapid Transit of 2030: Electrified, Automated, Connected" EBRT - Grant Agreement N. 101095882.

References

1. Aguiari, D., Chou, K.S., Tse, R., Pau, G.: Monitoring electric vehicles on the go. In: 2022 IEEE 19th Annual Consumer Communications & Networking Conference (CCNC), pp. 885–888. IEEE (2022)
2. Akiba, T., Sano, S., Yanase, T., Ohta, T., Koyama, M.: Optuna: a next-generation hyperparameter optimization framework. In: Proceedings of the 25rd ACM SIGKDD International Conference on Knowledge Discovery and Data Mining (2019)
3. Buller, S., Thele, M., Karden, E., De Doncker, R.W.: Impedance-based non-linear dynamic battery modeling for automotive applications. J. Power Sources **113**(2), 422–430 (2003)
4. Chen, Y., Tse, R., Bosello, M., Aguiari, D., Tang, S.K., Pau, G.: Enabling deep reinforcement learning autonomous driving by 3D-lidar point clouds. In: ICDIP 2022 (in press)
5. Chiu, K.C., Lin, C.H., Yeh, S.F., Lin, Y.H., Huang, C.S., Chen, K.C.: Cycle life analysis of series connected Lithium-ion batteries with temperature difference. J. Power Sources **263**, 75–84 (2014)

6. Chou, K.S., Aguiari, D., Tse, R., Tang, S.K., Pau, G.: Impact evaluation of driving style on electric vehicle battery based on field testing result. In: CCNC 2023 (in press)
7. Donkers, A., Yang, D., Viktorović, M.: Influence of driving style, infrastructure, weather and traffic on electric vehicle performance. Transp. Res. Part D: Transp. Environ. **88**, 102569 (2020)
8. dos Reis, G., Strange, C., Yadav, M., Li, S.: Lithium-ion battery data and where to find it. Energy AI **5**, 100081 (2021)
9. Doughty, D.H., Butler, P.C., Jungst, R.G., Roth, E.P.: Lithium battery thermal models. J. Power Sources **110**(2), 357–363 (2002)
10. Fang, K., Mu, D., Chen, S., Wu, B., Wu, F.: A prediction model based on artificial neural network for surface temperature simulation of nickel-metal hydride battery during charging. J. Power Sources **208**, 378–382 (2012). https://doi.org/10.1016/j.jpowsour.2012.02.059
11. Garche, J., Jossen, A.: Battery management systems (BMS) for increasing battery life time. In: Third International Telecommunications Energy Special Conference (IEEE Cat. No.00EX424), TELESCON 2000, pp. 81–88 (2000). https://doi.org/10.1109/TELESC.2000.918409
12. Golubkov, A.W., et al.: Thermal-runaway experiments on consumer Li-ion batteries with metal-oxide and olivin-type cathodes. RSC Adv. **4**(7), 3633–3642 (2014)
13. Guo, J., Li, Y., Pedersen, K., Stroe, D.I.: Lithium-ion battery operation, degradation, and aging mechanism in electric vehicles: an overview. Energies **14**(17), 5220 (2021)
14. Han, X., et al.: A review on the key issues of the lithium ion battery degradation among the whole life cycle. ETransportation **1**, 100005 (2019)
15. Jaliliantabar, F., Mamat, R., Kumarasamy, S.: Prediction of Lithium-ion battery temperature in different operating conditions equipped with passive battery thermal management system by artificial neural networks. Mater. Today Proc. **48**, 1796–1804 (2022)
16. Jiang, Y.H., Yu, Y.F., Huang, J.Q., Cai, W.W., Marco, J.: Li-ion battery temperature estimation based on recurrent neural networks. Sci. China Technol. Sci. **64**(6), 1335–1344 (2021). https://doi.org/10.1007/s11431-020-1736-5
17. Kane, M.: See a 2011 Nissan leaf battery dissected professionally: Video (2020). https://insideevs.com/news/390574/2011-nissan-leaf-battery-dissected-professionally/
18. Li, S.T., Cheng, Y.C.: A stochastic hmm-based forecasting model for fuzzy time series. IEEE Trans. Syst. Man Cybern. Part B (Cybern.) **40**(5), 1255–1266 (2009)
19. Liu, C., et al.: Phase change materials application in battery thermal management system: a review. Materials **13**(20), 4622 (2020)
20. Mc Carthy, K., Gullapalli, H., Ryan, K.M., Kennedy, T.: Electrochemical impedance correlation analysis for the estimation of Li-ion battery state of charge, state of health and internal temperature. J. Energy Storage **50**, 104608 (2022). https://doi.org/10.1016/j.est.2022.104608. https://www.sciencedirect.com/science/article/pii/S2352152X22006247
21. Neubauer, J., Wood, E.: Thru-life impacts of driver aggression, climate, cabin thermal management, and battery thermal management on battery electric vehicle utility. J. Power Sources **259**, 262–275 (2014)
22. Pesaran, A.A.: Battery thermal models for hybrid vehicle simulations. J. Power Sources **110**(2), 377–382 (2002)
23. Petneházi, G.: Recurrent neural networks for time series forecasting. arXiv preprint arXiv:1901.00069 (2019)

24. Raijmakers, L., Danilov, D., Eichel, R.A., Notten, P.: A review on various temperature-indication methods for Li-ion batteries. Appl. Energy **240**, 918–945 (2019)
25. Salcedo-Sanz, S., Deo, R., Carro-Calvo, L., Saavedra-Moreno, B.: Monthly prediction of air temperature in Australia and New Zealand with machine learning algorithms. Theor. Appl. Climatol. **125**(1), 13–25 (2016)
26. Smith, J., Singh, R., Hinterberger, M., Mochizuki, M.: Battery thermal management system for electric vehicle using heat pipes. Int. J. Therm. Sci. **134**, 517–529 (2018)
27. Talele, V., Thorat, P., Gokhale, Y.P., VK, M.: Phase change material based passive battery thermal management system to predict delay effect. J. Energy Storage **44**, 103482 (2021). https://doi.org/10.1016/j.est.2021.103482. https://www.sciencedirect.com/science/article/pii/S2352152X21011658
28. Wang, B., et al.: Study of non-uniform temperature and discharging distribution for Lithium-ion battery modules in series and parallel connection. Appl. Therm. Eng. **168**, 114831 (2020)
29. Xu, Z., Wang, J., Lund, P.D., Zhang, Y.: Estimation and prediction of state of health of electric vehicle batteries using discrete incremental capacity analysis based on real driving data. Energy **225**, 120160 (2021)